Predissociation processes in N2+ 2, O2+ 2, and NO2 + studied by ion kinetic energy spectroscopy

J. M. Curtis and R. K. Boyd

Citation: The Journal of Chemical Physics **81**, 2991 (1984); doi: 10.1063/1.448051
View online: http://dx.doi.org/10.1063/1.448051
View Table of Contents: http://scitation.aip.org/content/aip/journal/jcp/81/7?ver=pdfcov
Published by the AIP Publishing

Predissociation processes in N_2^{2+}, O_2^{2+}, and NO^{2+} studied by ion kinetic energy spectroscopy

J. M. Curtis and R. K. Boyd
Guelph-Waterloo Centre for Graduate Work in Chemistry, University of Guelph, Guelph, Ontario, Canada N1G 2W1

(Received 23 May 1984; accepted 14 June 1984)

Experimental values of kinetic energy release T, for predissociation processes of diatomic di-cations N_2^{2+}, O_2^{2+}, and NO^{2+} have been obtained using techniques of ion-kinetic-energy spectroscopy on a double-focusing mass spectrometer. Both unimolecular and collision-induced processes were studied. As a result, the present data confirm earlier work but include additional transitions not reported previously. Values of T obtained by entirely different technqiues are shown to be consistent with the present work when differences in energy resolution and experimental time window are considered. Attempts to correlate all available information on these diatomic di-cations (Auger, double-charge-transfer and kinetic-energy loss spectra, as well as appearance energy measurements) are hampered by lack of high-level *a priori* calculations of the potential curves.

INTRODUCTION

The standard expository monograph[1] and critical compilation of data[2] concerning the states of diatomic species agree on the paucity of experimental information available on diatomic di-cations XY^{2+}. Until comparatively recently, this was also true of theoretical investigations of these species. We have initiated a program of research designed to investigate predissociations of XY^{2+} species occurring on the microsecond time scale, by techniques of ion kinetic energy spectroscopy (IKES).[3] In addition, a parallel theoretical program has been undertaken[4,5] to produce potential energy curves using modern *ab initio* methods, together with quantitative calculations of energies and predissociation lifetimes of rotational-vibrational levels of these states. The aim is provide a self-consistent account of all available information on a given XY^{2+} species, drawn from IKES, Auger spectroscopy, double-charge-transfer translational spectroscopy, etc. Systems thus studied so far[3–5] are CH^{2+} and CO^{2+}.

In the present work, experimental IKES results are presented for predissociations of the species N_2^{2+}, O_2^{2+}, and NO^{2+}. These are compared with experimental data already in the literature, and in a general way with available theoretical treatments of these species. More detailed theoretical considerations are in progress, and will be reported separately.

EXPERIMENTAL METHODS

The apparatus used in the experimental work was a double-focusing mass spectrometer of conventional configuration (VG Analytical 7070F, magnetic sector radius 12.5 cm). The kinetic energy spectra were obtained using a scan of the accelerating voltage, with the electric sector and magnetic fields held fixed.[6] In this way, it is possible to investigate ion fragmentations occurring in the first field-free region, approximately 2–4 μs after formation of the precursor ions (e.g., N_2^{2+}) in the Nier-type ion source. An enclosed region located close to the ion source (focal point) slit serves as a collision-gas cell. The energy-resolving slit (intermediate focal point) is fully closeable, so that the energy resolution obtainable is limited by the energy spread in the primary ion beam (< 1.5 eV full width at half-maximum), and by the low

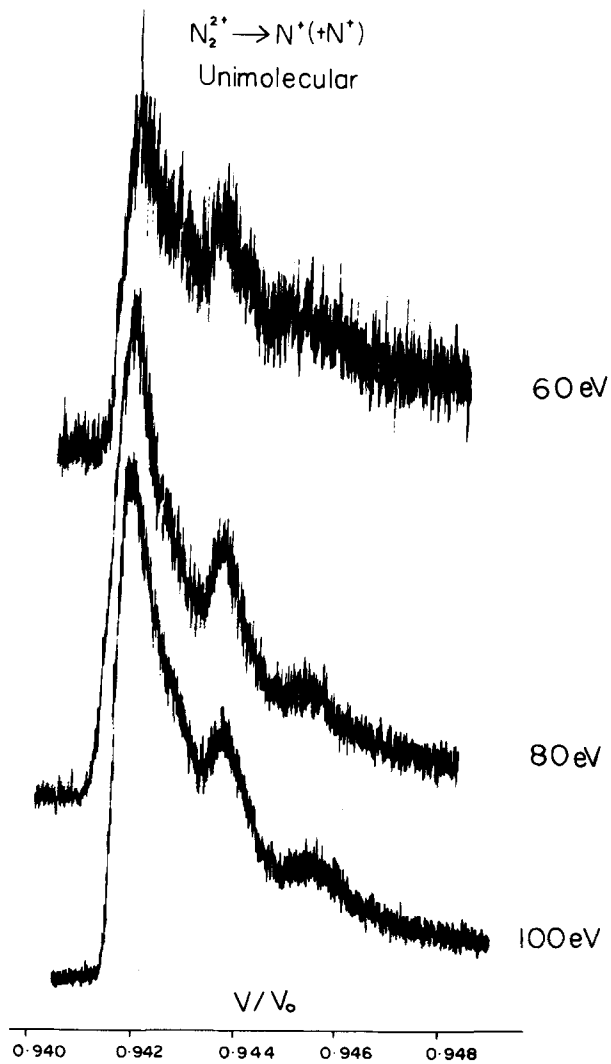

FIG. 1. Ion kinetic energy spectra of N^+ ions formed by unimolecular dissociations of N_2^{2+}. Only the high-energy side of the peak is shown.

 0021-9606/84/192991-11$02.10

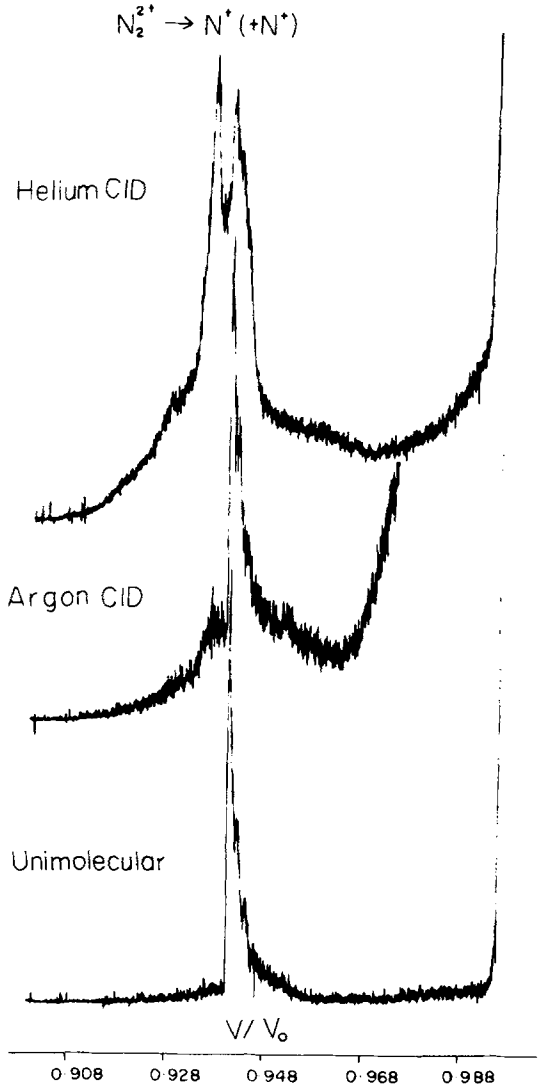

FIG. 2. Effect of helium and argon collision gas on ion kinetic energy spectrum (high-energy side only) arising from $N_2^{2+} \rightarrow 2N^+$.

degree of angular collimation particularly in the primary beam before fragmentation. This apparatus yielded acceptable data in the present instance, since fragmentations of doubly charged ions to two singly charged fragments invariably involve very large values of kinetic energy release. Together with operation of the so-called "amplification factor" arising[6] from the transformation from center-of-mass to apparatus-based coordinate systems, this permitted an effective energy resolution of about 0.1 eV in the experiments reported here.

RESULTS AND DISCUSSION

N_2^{2+}

A great deal of effort has been devoted recently to studies of the N_2^{2+} ion, which is of particular interest due to its potential importance for properties of the ionosphere.[7] In the present work, unimolecular dissociations of N_2^{2+} formed by electron impact have been studied on the time scale of approximately 2–4 μs after formation. In addition, dissociations induced by kilovolt collisions of N_2^{2+} ions with thermal gas targets have been investigated.

In Fig. 1 are shown kinetic energy spectra of N^+ ions formed by unimolecular dissociations (background pressure 2×10^{-8} Torr) of N_2^{2+}. The complete peak is deeply dished due to z discrimination.[6] The high-energy ions only are shown, the low-energy (backscattered) fragment ions forming a mirror image of the pattern shown in Fig. 1. Three well-resolved peaks, and one poorly resolved shoulder, can be distinguished, corresponding to kinetic energy release (T) values of 6.30 ± 0.05, 6.1–6.2 (unresolved shoulder), 5.95 ± 0.05 and 5.6 ± 0.08 eV. There appear to be no striking trends in variations of relative intensities with energy of the ionizing electrons. Unfortunately, limited signal-to-noise ratios prevent detection of any small differences in appearance energies.

A large-scale view of the high-energy side of unimolecular and collision-induced kinetic energy peaks is shown in Fig. 2. The main beam of unreacted ions is the extremely intense peak centered at $(V/V_0) = 1$. In addition, collision gases M induced dissociation processes preceded by electron transfer:

$$N_2^{2+}(\text{fast}) + M \rightarrow N_2^+(\text{fast}) + M^+ \rightarrow N^+ + N(+M^+). \quad (1)$$

These processes give rise to kinetic energy peaks also centered at $(V/V_0) = 1$, and are thus obscured by the main ion beam. However, additional peaks at larger kinetic energy release are clearly observed. Figures 3 and 4 show more detailed spectra for helium as collision gas, while Fig. 5 shows detail of the spectrum obtained using argon as collision gas. Both helium and argon give collision-induced peaks essentially identical with those observed in the unimolecular pro-

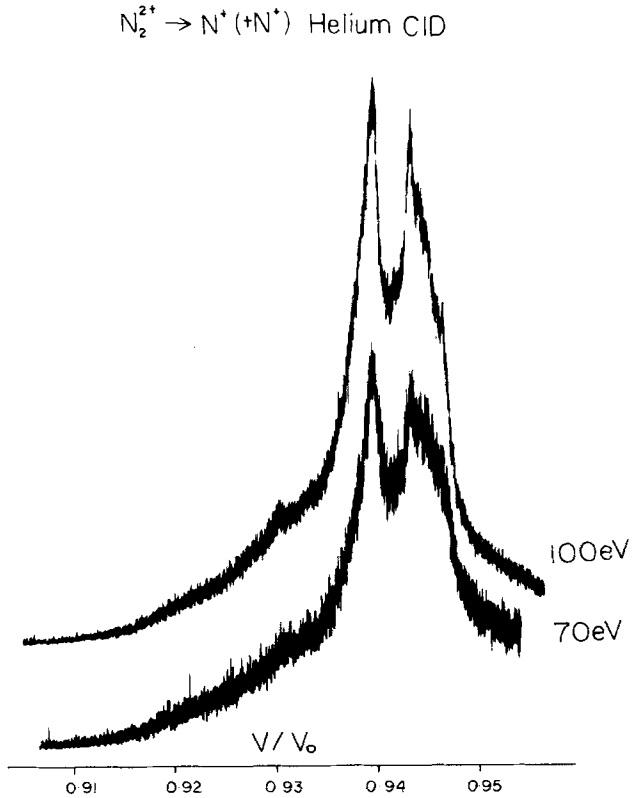

FIG. 3. Ion kinetic energy spectra for $N_2^{2+} \rightarrow 2N^+$ induced by collisions with helium.

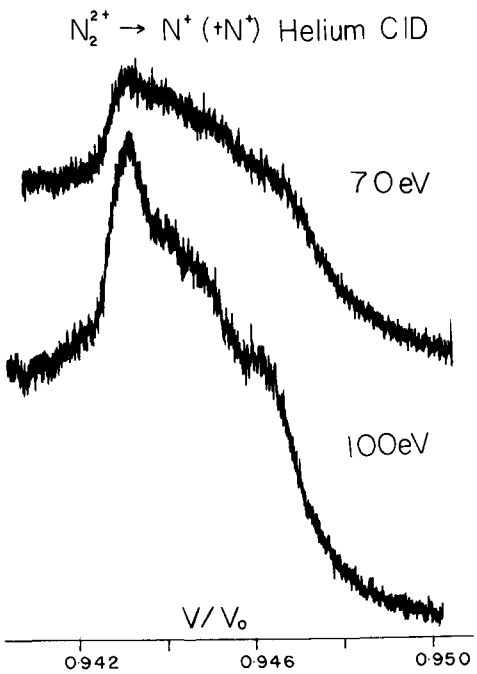

FIG. 4. Detailed view of helium collision-induced kinetic energy spectra for $N_2^{2+} \rightarrow 2N^+$.

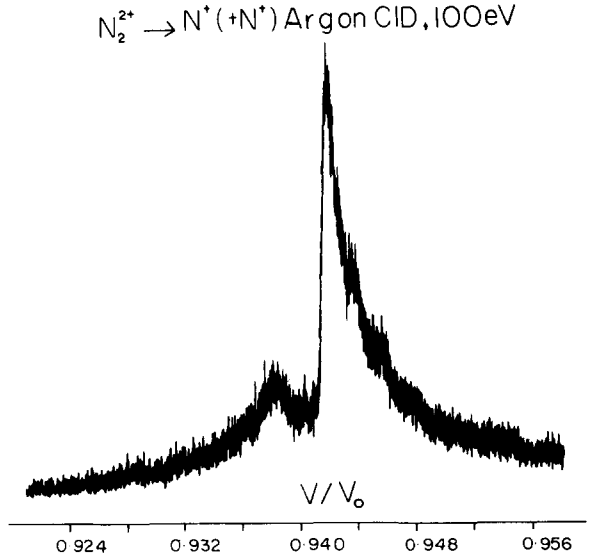

FIG. 5. Ion kinetic energy spectrum for $N_2^{2+} \rightarrow 2N^+$ induced by collisions with argon.

cess ($T = 6.3$, ~ 6.2, 5.9, and 5.6 eV), but also yield extra peaks. The sharp additional peak induced by collisions with helium corresponds to $T = 7.3 \pm 0.1$ eV. This sharp structure, characteristic of a narrow range of values of T, is underlain by a broader feature which is clearly visible in the spectrum induced by collisions with argon, from which the additional sharp peak induced by helium collisions is absent. The maximum of the broader peak corresponds to $T = 7.1 \pm 0.1$ eV. An additional collision-induced peak with $T = 9.4 \pm 0.2$ (helium) and 9.6 ± 0.2 eV(argon) can also be seen (rather weak in the argon case).

These data are summarized in Table I, together with comparable literature data. The discrepancies between at least some of these data have been discussed recently.[14] The early work of Beynon *et al.*,[8] who studied the unimolecular process using techniques identical to those of the present work, is in excellent agreement with the present data but apparently did not resolve the finer structure at lower values of T. Franklin and Haney[9] exploited the peak broadening, due to fragmentations occurring in a time-of-flight mass spectrometer, to estimate a value of $T = 8$ eV. Such determinations[9] are of low precision compared with the methods used here, and in the present case were stated[9] to be subject to interference from other processes. However, this work[9] did manage to establish a reliable appearance energy for the $N_2^{2+} \rightarrow 2N^+$ process observed, which together with the value of T permitted the identification of the N^+ fragments as the ground-state ^3P ions.

Schultz *et al.*[10] studied collision-induced fragmentations of N_2^+ ions, using a focusing parabola analyzer. The angular dependence of the fragment-ion kinetic energy spectrum was determined,[10] but the kinetic energy resolution was low. The collision-induced process studied was identified via measurements of both T and of kinetic-energy loss, which were shown[10] to be consistent with $N_2^+ \rightarrow N_2^{2+}(+e^-) \rightarrow 2N^+$. It is likely that the broad peak interpreted in this way[10] is an unresolved envelope of Fig. 3.

Deleanu and Stockdale[11] used an apparatus incorporating crossed molecular and electron beams, with time-of-flight analysis of the N^+ ion products. The various ion groups thus observed[11] were subject to interpretation, and those included in Table I were assumed[11] to arise from N_2^{2+} because of the large values of T thus found. These data are of low precision, but are in fair agreement with more recent data discussed below. Further, an appearance energy of approximately 50 eV was established[11] for the ion group with $T = 6$–8 eV. Later work by Stockdale[12] used techniques to detect the two N^+ fragments in coincidence, thus unambiguously identifying N_2^{2+} as the precursor. These later results[12] have been stated[13,14] to be in poor agreement with the earlier work[11] and with other coincidence-detection data. The values quoted in Table I are those quoted in the original work[12] as being "...possible peaks near 6.2 and 8 eV N^+ kinetic energy...". This statement was interpreted previously[13,14] as implying that the values of T must be *twice* the quoted values, which are apparently per N^+ fragment. However, later in Stockdale's paper[12] it is stated that a similar indication of two peaks near 6 and 8 eV is present in a 150 eV electron impact N^+ kinetic energy spectrum obtained previously[11] in the same apparatus. In fact, these latter data are presented in the original work[11] as N^+ ion groups peaking near 3 to 4 eV, thus (when doubled) giving rise to T values of approximately 6 and 8 eV. Therefore, it is presently considered that the coincidence work of Stockdale[12] is in general agreement with the other data of Table I. The discrepancies noted previously[13,14] probably reflect an unfortunate ambiguity in the presentation of data.[12]

The two more recent studies of the unimolecular process $N_2^{2+} \rightarrow 2N^+$, which used coincidence techniques,[13,14] are in fair agreement with one another although a constant difference of about 0.7 eV between the two sets of T values is

TABLE I. Values of kinetic-energy release T for $N_2^{2+} \rightarrow 2N^+$.

Observed process	Time window	T (eV)	A.E. (eV)	Expt. method	Reference
$N_2^{2+} \rightarrow 2N^+$, unimolec.	~2–4 μs	6.22	...	Metastables	8
$N_2 \xrightarrow{He} + e^- \rightarrow 2N^+(^3P) + 3e^-$	~0–few μs	8.0	47.0	Metastables	9
$N_2^+ \rightarrow 2N^+ + e^-$	~0–few μs	6.7	...	Collision	10
$N_2 + e^- \rightarrow N^+(+N^+) + 3e^-$	~0–few μs	6–8	~50	Time of flight	11
		~14	...		11
$N + {}^2_2 \rightarrow 2N^+$ (unimolec)	~0–few μs	~6	...	Coincidence	12
		~8	...	Spectroscopy	12
$N_2^{2+} \rightarrow 2N^+$ (unimolec)	~0–3 μs	~7	47.3	Coincidence	13
		9.7	...	Spectroscopy	13
		14	...		13
$N_2 \xrightarrow{1\ MeV\ He^+} 2N^+$	0–1 μs	7.8	...	Coincidence	14
		10.2	...	Spectroscopy	14
		14.8	...		14
$N_2^{2+} \rightarrow 2N^+$, unimolec.	~2–4 μs	6.30	...	Metastables	Present
		6.1–6.2	...		work
		5.95	...		
		5.6	...		
$N_2^{2+} \xrightarrow{He} 2N^+$	~0–2 μs	9.4	...	Collision	Present
	after collision	7.3	...		work
		6.3	...		
		6.2	...		
		6.0	...		
		5.7	...		
$N_2^{2+} \xrightarrow{Ar} 2N^+$	~0–2 μs	9.6	...	Collision	Present
	after	7.1	...		work
	collision	6.3	...		
		6.1–6.25	...		
		5.9	...		
		5.6	...		

apparent (Table I). The earlier work of Brehm and de Frenes[13] used electron impact ionization, and a retardation technique for kinetic energy analysis which requires differentiation of the observed response curves to obtain the kinetic energy spectra. Such methods are susceptible to inaccuracies, and the kinetic energy resolution obtained[13] was low. The most recent coincidence work due to Edwards and Wood[14] used direct kinetic energy analysis which yielded kinetic energy peaks whose width at half-height was approximately 1 eV.

A parameter which is of considerable importance in comparisons such as those of Table I is the time window, following formation of the N_2^{2+} precursor, over which the fragmentations are observed. Thus, in the mass spectrometric methods used here and previously,[8] the "metastable window" is reasonably well defined (2 to 4 μs), and discriminates strongly against unimolecular processes occurring with a half-life shorter than about 0.05 μs or longer than about 100 μs. Collision-induced processes studied by such techniques,[6] however, occur within the time window from zero to approximately 2 μs after the collisional activation event, which in turn occurs approximately 2 μs after formation of the N_2^{2+}. The various coincidence experiments[12–14] included in Table I sample shorter dissociative lifetimes,[12] from approximately zero to 1 μs, and the results are possibly dominated by the much faster events.

Thus, when differences in energy resolution and in observation time window are taken into account, the observations listed in Table I are in much better agreement with one another than appears at first sight. Those techniques which sample faster dissociation events yield kinetic energy spectra with resolved features at considerably higher values of T than those revealed by the present techniques, though the use of collision gas in the present work provides a bridge to the other methods (Table I).

The energy threshold for the net process (2):

$$N_2(^1\Sigma_g^+, v = 0) \rightarrow 2N^+(^3P) \tag{2}$$

is 38.84 eV. Several determinations[15–17] have been made of the vertical appearance energy of N_2^{2+} ions stable on the mass spectrometer time scale (few μs), yielding an average value of 42.8 $\pm$ 0.3 eV for the electron-impact induced process. This should be compared with the appearance energy $\gtrsim$ 47 eV for two N^+ fragment ions from N_2^{2+} (Table I). Other important information is obtained from Auger spectroscopy[18–20]; the three independent investigations are in excellent agreement with one another, although one of them[18] was able to resolve some finer detail than the others. An important finding in the Auger work[18–20] is that the lowest state of N_2^{2+} identified as arising from a "normal" Auger transition (i.e., K-WW in the notation described previously,[20] devoid of shake-up or shake-off processes), lies about

TABLE II. Bound states of N_2^{2+} from calculations due to Taylor.[a]

State[b]	Dissociated limits[c]	T_e(eV)[d]	D_{eff}(eV)[e]	r_e(nm)	E(inner)(eV)[f]	E(outer)(eV)[f]
$X\,^1\Sigma_g^+$	$N^+(^3P)+N^+(^3P)$	0	2.5	0.1139	4.1	4.0
$A\,^1\Pi_u$	$N^+(^3P)+N^+(^3P)$	2.3	1.1	0.1266	7.9	6.5
$2\,^1\Sigma_g^+$	$N^+(^3P)+N^+(^3P)$	2.6	1.2	0.138	9.4	7.4
$D\,^1\Sigma_u^+$	$N^+(^1D)+N^+(^1S)$	9.1	1.9	0.1140	9.2	9.1
$a+\,^3\Pi_u$	$N^+(^3P)+N^+(^3P)$	0.6	2.2	0.1254	6.3	4.9
$b\,^3\Sigma_g^-$	$N^+(^3P)+N^+(^3P)$	1.5	0.9	0.1379	8.7	6.9
$c\,^3\Sigma_u^+$	$N^+(^3P)+N^+(^3P)$	1.5	2.4	0.1109	5.6	5.6

[a] Reference 29.
[b] Labeling of states used by Taylor (Ref. 29) differs from earlier work.
[c] $N^+(^1D)+N^+(^1S)$ lies 5.95 eV above $N^+(^3P)+N^+(^3P)$.
[d] Potential minimum of $X\,^1\Sigma_g^+$ state taken as 42.8 eV above $v=0$ of $X\,^1\Sigma_g^+$ state of N_2 and thus 4.0 eV above $N^+(^3P)+N^+(^3P)$.
[e] Energy difference between potential maximum and minimum.
[f] Relative to $N^+(^3P)+N^+(^3P)$ dissociation limit, which in turn lies 38.84 eV above $v=0$ level of $X\,^1\Sigma_g^+$ state of N_2, and 4.0 eV below $v=0$ of $X\,^1\Sigma_g^+$ state of N_2^{2+}. E(inner) refers to E at inner limit of Franck–Condon region, E(outer) to outer limit.

42.8 eV above the ground state of N_2. This is in excellent agreement with the mass spectrometric appearance energy, in marked contrast with the analogous situations[3,5] for CO where the lowest Auger line[18] is at least 1 eV below the appearance energy.

Other relevant optical experiments include observation[21] of a headless emission band in a hollow-cathode discharge in N_2, subsequently[22] assigned to a transition between states of N_2^{2+}. Photoabsorption cross sections for N_2, with photon energies in the range 20–100 eV, have been described.[23,24] As for the other gases thus studied,[23,24] a broad maximum is observed at photon energies close to the appearance energy for N_2^{2+} measured[15–17] by mass spectrometric methods. Finally, double-charge-transfer translational spectroscopy experiments,[25] which measure the energy required for the process (3):

$$N_2 + H^+(\text{fast}) \rightarrow N_2^{2+} + H^-(\text{fast}) \qquad (3)$$

have yielded information on low-lying singlet states of N_2^{2+}.

Interpretation of all of this information in a self-consistent fashion will require a major effort. The corresponding problem[3,5] for CO^{2+} is appreciably simpler, since the density of electronic states is much smaller for CO^{2+} than for N_2^{2+}. In turn, this is due partly to nuclear symmetry in the latter case (gerade and ungerade states), but more importantly to the high density of states for N^+ (isoelectronic with neutral carbon atoms) compared with C^+ and O^+. Any such comprehensive interpretation will depend upon the availability of highly reliable *ab initio* calculations of potential curves for N_2^{2+}. Theoretical calculations available in the literature range from the early ingenious semiempirical procedures due to Hurley[26,27] to more recent *ab initio* calculations. The latter include a full valence configuration interaction treatment in a minimal basis set,[28] and single-configuration self-consistent field calculations using a much larger basis set.[7] The limitations inherent in these approaches have been emphasized by Taylor,[29] who undertook an ambitious complete-active-space self-consistent field computation for N_2^{2+}. This recent work[29] appeared when similar work had already been initiated by ourselves, in a fashion similar to that already completed[5] for CO^{2+}. The degree of detail reported by Taylor[29] is insufficient for our purposes, and our attempt to provide a comprehensive interpretation for N_2^{2+} will be reported separately. Here, we restrict ourselves to tentative assignments of the observed T values (Table I), along the lines described recently.[14]

The pertinent properties of the bound states of N_2^{2+}, characterized by the *a priori* calculations of Taylor,[29] are summarized in Table II. The potential minimum of the $X\,^1\Sigma_g^+$ state lies within the Franck–Condon region,[29] and is assumed to correspond to the N_2^{2+} ions observed[15–17] at threshold. The only predissociations observed to occur on a delayed time scale (approximately 2–4 μs after formation) are the unimolecular processes observed in the present work and previously[8] (Table I). These transitions have the appearance of a vibrational progression, with the varying vibrational spacings anticipated for the levels near the potential maximum of a typical XY^{2+} bound state. If the delayed predissociation processes correspond to tunneling, it is known in the case[5] of CO^{2+} that the rotational-vibrational levels with appropriate lifetimes (few μs) lie at energies close to the maximum of the zero-angular-momentum potential curve. This maximum energy can be deduced from Table I, relative to the $N^+(^3P)+N^+(^3P)$ limit, as $(4.0+T_e+D_{eff})$ eV, where 4.0 eV is the difference between the appearance energy for stable N_2^{2+} (assumed to be ground-state N_2^{2+}) and $2N^+(^3P)$. For the $a\,^3\Pi_u$ state, the energy at the maximum is 6.8 eV, for example. This state is the most likely candidate, of all of Taylor's bound states,[29] to account for the delayed predissociations in terms of a tunneling mechanism (Herzberg case I). No other state in Table II even approaches the appropriate combination of properties. This is reassuring, since the higher triplet states are likely to have decayed radiatively within the 2 μs or so available.

If the delayed predissociation corresponds to "forbidden" electronic predissociation (Herzberg case III[1]), the most likely selection rule to be thus violated is $\Delta S=0$. It is necessary, therefore, to look for singlet–triplet crossings for N_2^{2+} accessible by Franck–Condon transitions from ground-state N_2, at about 5.9–6.3 eV above $N^+(^3P)+N^+(^3P)$. The closest candidate would be the predissociation of the $A\,^1\Pi_u$ state by the $b\,^3\Sigma_g^-$ state, but such a

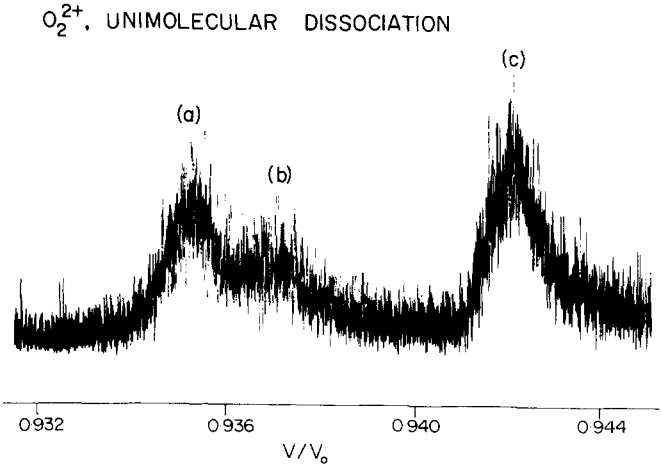

FIG. 6. Ion kinetic energy spectrum of O^+ ions formed by unimolecular dissociations of O_2^{2+}. Only the high-energy side of the peak is shown.

predissociation is rigorously forbidden[1] by the $s \leftrightarrow a$ selection rule. Thus, insofar as the theoretical curves due to Taylor[29] are concerned, no suitable electronic mechanism for the delayed predissociation can be found. Note however that almost all of Taylor's states[29] (both bound and unbound) correlate at long range with the ground-state fragments $2N^+(^3P)$. In view of the density of states for N^+ (^3P, ^1D, ^1S lying at 0, 1.90, and 4.05 eV, respectively), many other singlet–triplet crossings must exist.

All other experimental measurements summarized in Table I involve observation of predissociation events at very short times. Thus, transitions to repulsive curves can be invoked to account for these. Again using Taylor's curves[29] as the best presently available, we seek potential curves which, within the Franck–Condon region, lie at 7–8, 9.5–10.5, and 14 eV above the dissociation limits. Note (Table I) that helium collisions induce *two* types of dissociative transitions, one giving a sharp peak (narrow range of values of T) with $T = 7.3$ eV, and the other (also induced by collisions with argon) a broad peak (considerable range of values of T), with $T = 7.1$ eV. The broad peak could correspond to collision-induced transition of normally stable N_2^{2+} ions to a repulsive portion of a potential curve, well above any quasibound region (process 1 in the classification due to Durup[30]). Possibilities among Taylor's curves[29] include the $A\ ^1\Pi_u$ state and the $b\ ^3\Sigma_g^-$ state, both of which possess extensive energy ranges at the appropriate height above the $2N^+(^3P)$ limit, and within the Franck–Condon region. (The $^1\Pi_u$ state was formerly assigned[14] to a process with $T = 7.8$ eV.) If such an interpretation of the broad feature (Figs. 3–5) is valid, a kinetic energy loss is presumably involved. This would show up in the present experiments as an asymmetry, about $(V/V_0) = 1$, of high-energy (Figs. 1–5) and low-energy "horns" of the ion kinetic energy peaks. We were unable to detect any such asymmetry in the present work, but our instrumental stability was low enought that, in the time required to scan through both horns, considerable instrumental drift could have occurred. The alternative explanation of this broad feature would be electronically adiabatic dissociation of some state(s) of N_2^{2+} via rotational-vibrational excitation (process 2 of Durup[30]), consistent[30,31] with the fact that argon is an efficient collision partner for this process.

The sharp collision-induced peak at $T = 7.3$ eV (Fig. 3) must correspond to some much more well-defined process, since the range of values of T must be narrow. In addition, only helium collisions were observed to induce this process. The unique properties of helium as collision partner in studies of this type have been noted previously.[30,31] In view of the wide spacing between states of He, it is unlikely that collision-induced electronic curve crossing via a triatomic collision complex is responsible. Further information from both theory and experiment seems necessary for the reliable interpretation of these observations.

The fast processes with $T = 9$–10 eV (Table I) can be accounted for by Franck–Condon ionization of N_2 to any or all of repulsive regions of the $^1\Delta_g$, $2\ ^1\Sigma_g^+$, $^3\Sigma_g^-$, or $^3\Pi_g$ states located by Taylor.[29] The two singlet states appear to fit the requirements slightly better, and indeed these were the states, as characterized by Thulstrup and Andersen,[28] assigned previously.[14] The fast process with $T = 14.5$ eV (Table I) is consistent with Franck–Condon ionization of N_2 to the wholly repulsive $^1\Sigma_u^-$ state[29] correlating with $2N^+(^3P)$ (again assigned previously[14] on the basis of earlier calculations[28]), or to the $^3\Delta_u$ repulsive state correlating with the same dissociation limits. The repulsive $^3\Delta_g$ state,[29] which crosses the Franck–Condon region between about 15 to 16.5 eV, correlates with $N^+(^3P) + N^+(^1D)$ and would thus give rise to $T = 13$ to 14.5 eV.

In summary, despite the fact that the energy scale of Taylor's *a priori* calculations[29] for N_2^{2+} can be fairly unambiguously established (unlike the case[5] of CO^{2+}), interpretation of the ion kinetic energy information (Table I) is disappointingly imprecise. This undoubtedly reflects the much greater density of states for N_2^{2+} than for CO^{2+}. Further theoretical and experimental work on this problem is in progress.

O_2^{2+}

The O_2^{2+} ion is also of considerable interest in aeronomy. The experimental ion kinetic energy spectra (Figs. 6 and 7) obtained in the present work are of appreciably poorer quality than the corresponding spectra for N_2^{2+}. This is due to limited filament life in an ion source with pure O_2 used as the sample gas. The values of T are collected in Table III, together with comparable data obtained previously.[8,13] The ion kinetic energy spectrum for $O_2^{2+} \rightarrow 2O^+$, obtained[13] by differentiation of the retarding field curve, is of very low resolution; the values of T from this work,[13] quoted in Table III, represent the three broad maxima in the differentiated curve.

Other experimental information available on O_2^{2+} include several determinations[15,16,31] of the electron-impact appearance energy of O_2^{2+} from O_2. The values thus obtained (36.3 ± 0.5, 37.2 ± 0.5, and 35.6 ± 0.3 eV) are not in very good agreement with one another, but may be represented by an average value of 36.4 ± 0.7 eV. The Auger spectra[18,20] of O_2 are subject to difficulties of interpretation, due to spin coupling of the K shell electron in the intermediate K hole ion O_2^{K+} with uncoupled electrons in the partially filled

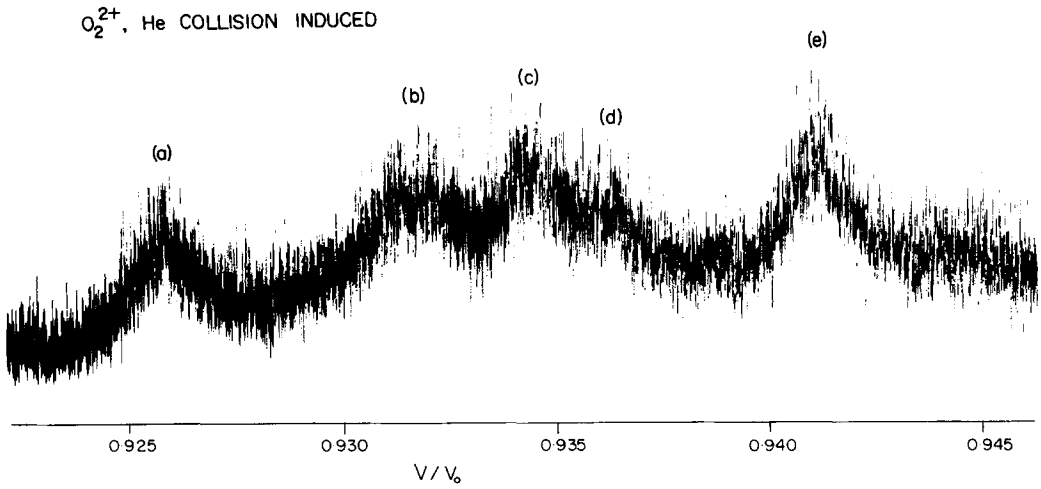

FIG. 7. Ion kinetic energy spectrum for $O_2^{2+} \rightarrow 2O^+$ induced by collisions with helium.

$2p\Pi_g$ orbital. This gives rise to two states of O_2^{K+} separated by about 1.1 eV, and thus to doublets in the Auger spectrum corresponding to transitions to the same final states of O_2^{2+}. The lowest energy level of O_2^{2+} thus detected in the Auger spectra[18,20] lies about 37.5 eV above the $X\,^3\Sigma_g^-$ ground state of O_2. The maximum intensity of this Auger line[20] lies at approximately 38.3 eV. Thus despite the considerable uncertainties in the experimental data, there does appear to be a definite tendency for the electron-impact threshold for O_2^{2+} to be observed at lower values than that for Auger transitions. This possibly reflects only differing sensitivities for detection. In the case[5] of CO^{2+}, for which the experimental reproducibility is considerably better, the Auger onset was found to be significantly below that for electron impact, a much more difficult observation to explain.[5]

Other maxima in the Auger spectra, which were identified[20] as the expected 1.1 eV doublets, were observed at 42.8 (doublet lines B 4 and B 5[20]), 48.6 (B 8 and B 9), and 51.4 eV (B 10 and B 11) above the ground state of O_2. The first two of these agree well with observation by double-charge-transfer spectroscopy[25] of two triplet states of O_2^{2+} at 43.0 ± 0.5 and 48 ± 1 eV. The high-energy-photon absorption data[23,24] show a broad unresolved absorption at 35–40 eV photon energy.

Theoretical treatments of O_2^{2+} include the semiempirical calculations of Hurley,[27] and an *a priori* calculation by Beebe, Thulstrup, and Andersen[33] at about the same level as that[28] discussed above for N_2^{2+}. This theoretical work[33] is the best available for O_2^{2+}, but is subject to the reservations expressed previously,[29] concerning the limited basis set.

A notable feature of the ground state of O_2^{2+} ($X\,^1\Sigma_g^+$) is that the calculated[33] value of r_e is shorter (0.1174 nm) than that for the $X\,^3\Sigma_g^-$ state of O_2 (0.1278 nm calculated,[33] 0.1208 nm experimental[1]). This can be understood qualitatively on the basis of rudimentary molecular orbital theory, which predicts a ground-state configuration for O_2 of $(KK)(2s\sigma_g)^2(2s\sigma_u)^2(2p\sigma_g)^2(2p\Pi_u)_4(2p\Pi_g)^2$. The outermost orbital is expected[1] to be strongly antibonding, so that removal of the two electrons occupying this orbital should strengthen and thus shorten the bond. This simple picture does not account for the participation of charge-polarization states, but clearly the ground state of O_2^{2+} is expected to have a smaller r_e value[33] than that of O_2.

Unfortunately, Beebe *et al.*[33] gave very few details of the results of their calculations on O_2^{2+}, and published rather small diagrams of their potential curves. Accordingly, much of the data listed in Table III are correspondingly uncertain, being estimated from these published diagrams.[33] The pre-

TABLE III. Values of kinetic energy release T for $O_2^{2+} \rightarrow 2O^+$.

Observed process	Time window	T(eV)	A.E.(eV)	Exptl. method	Reference
O_2^{2+}, unimolec.	~2–4 μs	8.03	···	Metastables	8
$O_2^{2+} \rightarrow 2O^+$, unimolec.	~2–4 μs	6.7	···	Metastables	Present
		7.9	···		work
		8.4	···		
$O_2^{2+} \xrightarrow{He} 2O^+$	~0–2 μs	6.8	···		
	after	8.0	···	Collision	Present
	collision	8.5	···		work
		9.2	···		
		10.9	···		
$O_2^{2+} \rightarrow 2O^+$, unimolec.	~0–3 μs	7	40.2	Coincidence	13
		11		spectroscopy	
		16			

TABLE IV. Bound states of O_2^{2+} from calculations due to Beebe *et al.*[a]

State	Dissociated limits[b]	T_e(eV)[c]	D_{eff}(eV)[d]	r_e(nm)	E(Franck–Condon) (eV)[e]
$^1\Sigma_g^+$	$O^+(^4S)+O^+(^4S)$	0	0.8	0.1174	36.7
$^3\Pi_g$	$O^+(^4S)+O^+(^2D)$	5.9	0.2	0.1291	42.4
$^3\Sigma_u^-$	$O^+(^4S)+O^+(^2P)$	5.8	0.1	0.1458	42.6
$^1\Sigma_u^-$	$O^+(^2D)+O^+(^2D)$	6.9	0.6	0.1418	43.5
$^1\Pi_g$	$O^+(^2D)+O^+(^2D)$	7.4	1.1	0.1271	43.8
$^1\Delta_u$	$O^+(^2D)+O^+(^2D)$	7.8	1.0	0.1393	44.6
$^1\Sigma_g^+$	$O^+(^2D)+O^+(^2D)$	7.1	0.4	0.152	45.5

[a] Reference 33.
[b] $2\,O^+(^4S)$ lies at 32.4 eV above $v=0$ level of $X\,^3\Sigma_g^-$ state of O_2. $O^+(^2D)$ and $O^+(^2P)$ lie 3.32 and 5.02 eV, respectively, above $O^+(^4S)$.
[c] Potential minimum of $X\,^1\Sigma_g^+$ state of O_2^{2+} taken as 36.4 eV above $v=0$ level of $X\,^3\Sigma_g^-$ state of O_2, and thus 4.0 eV above $2\,O^+(^4S)$.
[d] Difference between potential maximum and minimum.
[e] Intersection of potential curve with $r=0.1278$ nm, the value for r_e for $X\,^3\Sigma_g^-$ state of O_2 calculated in same fashion as O_2^{2+} states. Energies relative to ground state of O_2.

dissociation process with $T=6.7$ eV (Table III) fits nicely with that predicted for $O_2^{2+}(^3\Pi_g)\rightarrow O^+(^4S)+O^+(^2D)$ via tunneling predissociation. This lowest bound triplet state ($^3\Pi_g$) is probably also that observed in the double-charge-transfer experiment[25] and in the Auger spectrum.[20]

According to the theoretical procedures of Hurley,[27] the lowest bound triplet state is a $^3\Sigma_u^+$ state correlating with $2O^+(^4S)$. However, Beebe *et al.*[33] find that this low-lying triplet state is *not* bound. This is unfortunate since this state as characterized by Hurley[27] is a likely candidate for tunneling predissociation with $T=7.5$–8 eV, as observed (Table III). The delayed predissociation with $T=8.4$ eV (Table III) does not appear to be interpretable in terms of tunneling from any state characterized by either calculation.[27,33] These two delayed processes possibly correspond to electronic predissociation of radiationally stable states by curve crossing with repulsive states of different multiplicity. These "forbidden" transitions with $\Delta S\neq 0$ could well proceed on a microsecond time scale.[1] For example, the $^1\Sigma_u^-$ state (Table IV) will not undergo a radiative transition to the $^1\Sigma_g^+$ ground state, but is crossed[33] in the Franck–Condon region by the lowest $^3\Pi_u$ state correlating with $O^+(^4S)+O^+(^2D)$. The predicted value of T is thus 7.8 eV, in good agreement with one of the experimentally observed values (Table III).

The larger values of T (Table III) observed on shorter time scales are even more difficult to interpret, since in the region of interest the potential curves of Beebe *et al.*[33] are generally extremely steep. The case of O_2^{2+} clearly requires a theoretical contribution at a level comparable with that achieved by Taylor[29] for N_2^{2+}.

NO^{2+}

An extremely weak peak due to the $NO^{2+}\rightarrow O^+(+N^+)$ unimolecular transition was observed (Fig. 8), with $T=6.1$ eV in good agreement with the previous value[8] for this delayed dissociation. Use of argon as collision gas made essentially no difference to the observed peak, but did produce an additional central feature due to dissociation preceded by electron transfer:

$$NO^{2+}\xrightarrow{Ar}NO^+(+Ar^+)\rightarrow O^+(+N).$$

Such processes have been observed previously[3] for CO^{2+}. Helium collision gas also yielded similar peaks (Fig. 8), but in

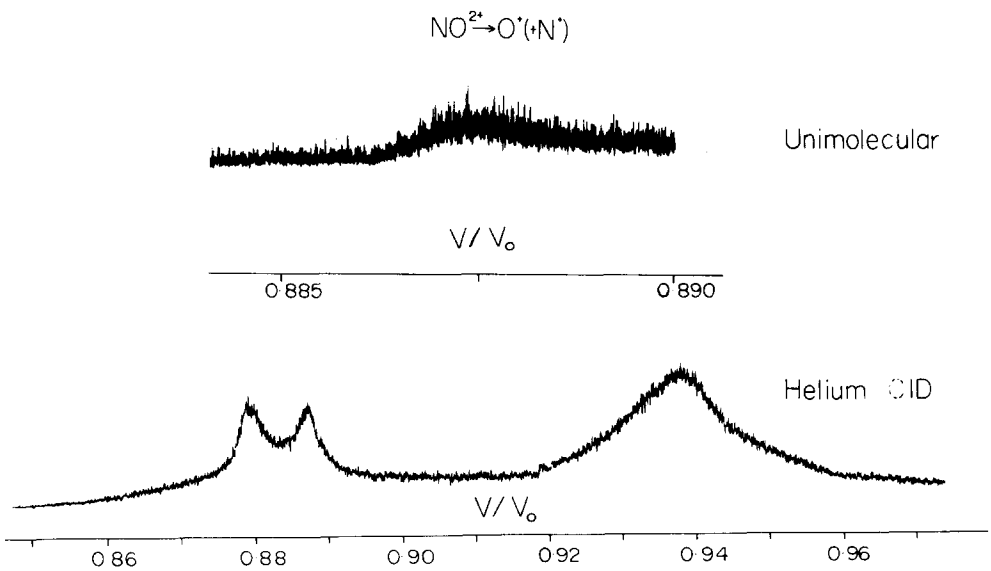

FIG. 8. Ion kinetic energy spectra (high-energy horns only) for $NO^{2+}\rightarrow O^+(+N^+)$. Broad central peak, induced by collisions with He, corresponds to dissociation preceded by charge transfer $NO^{2+}(\rightarrow NO^+)\rightarrow O^+(+N^+)$.

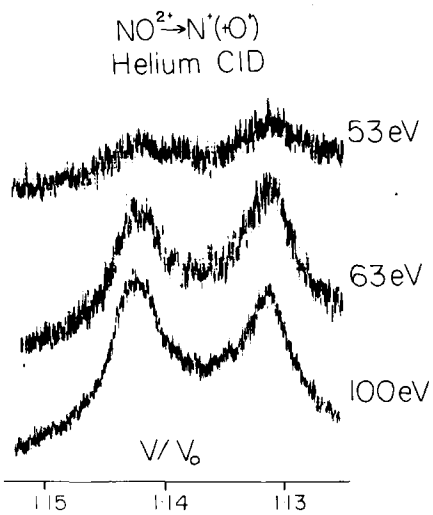

FIG. 9. Ion kinetic spectra for $NO^{2+} \rightarrow N^+(+O^+)$ induced by collisions with helium, as function of ionizing electron energy.

addition greatly accentuated the direct dissociation of NO^{2+} into two ions. The process with $T = 6.1$ eV is now much more intense, and an additional process with $T = 8.1$ eV is induced by collisions with helium. As a check, the N^+ fragment ions were also recorded, and their kinetic energy spectra are shown in Fig. 9 as a function of ionizing electron energy. No reliable appearance energies can be deduced, but it is clear that the process with $T = 8.1$ eV has a higher appearance energy than that with $T = 6.1$ eV. The only other comparable report in the literature is that due to Brehm and de Frenes,[13] who used coincidence detection together with retardation analysis of the ion kinetic energies. The differentiated retardation curve[13] is extremely broad, extending from $T = 5$ eV to $T = 23$ eV with a badly defined maximum near 8.5 eV. The appearance energy for $N^+ + O^+$ ion pairs was determined[13] to be 40.3 eV.

The appearance energy for NO^{2+} ions stable on the mass spectrometer time scale has been determined using electron impact methods.[34–36] The most recent determination[36] appeared to exhibit a well-defined break in the ionization efficiency curve, corresponding to separated ionization energies of 39.3 and 41.2 eV. Alternatively, if this discontinuity was ignored a best value of 40.3 ± 0.3 eV was obtained.[36] This is to be compared with the earlier work,[34,35] which yielded values of 39.8 ± 0.3 and 38.3 ± 0.5 eV, respectively. The first of these[34] is in agreement with the most recent work,[36] but the second[35] seems significantly low.

The Auger spectra[18,20] of NO are complicated both by the fact that the spectra excited by K-hole ions centered on both N and O do not agree well, and by coupling of the $1s$ electron in the K-hole ion with the unpaired electron in the $2p\pi^*$ molecular orbital. This spin coupling gives rise to singlets and triplets, with a separation of 1.5 eV in the Auger lines in the case of nitrogen, and 0.7 eV for oxygen.[18] The relative population of triplet to singlet states should be close to three to one, which together with the anticipated splittings provides a crucial test for lines assigned as normal Auger transitions. The Auger lines designated[20] B 1 and B 2 meet all criteria for normal transitions, and correspond to a state of NO^{2+} with a maximum intensity at 37 eV above the $v = 0$ level of the $X\,^2\Pi$ state of NO and an onset at about 35.5 eV. Both of these lie appreciably below the appearance energies derived from electron-impact ionization efficiency curves.[34–36] This discrepancy is very similar to that noted previously[5] for CO.

The double-charge-transfer spectra[25] show three peaks corresponding to doublet states of NO^{2+}. The energies of these states, relative to the ground state of NO, are, respectively, 39.3 ± 0.5, 42.4 ± 1.0, and 47.2 ± 0.5 eV. The first of these is in fair agreement with the electron impact appearance energy results,[36] and presumably corresponds to the ground state of NO^{2+}. In the original work,[25] this peak at 39.3 eV was assigned to transitions to both the $X\,^2\Sigma^+$ and the $A\,^2\Pi$ states of NO^{2+} as characterized by the theoretical procedure of Hurley.[27] The peak at 42.4 eV was assigned[25] to the $B\,^{2+}\Sigma^+$ state,[27] and that at 47.2 eV to higher doublet states not described by Hurley's procedure[27] since corresponding information on CN is not available.

More recently,[37] translational energy-loss spectroscopy has been applied to NO^{2+} ions which undergo collisions several μs after formation and thereafter survive as NO^{2+} for another few μs. Kinetic-energy-loss peaks were observed[37] at 1.7 and 4.8 eV. In view of the experimental conditions, the precursor ions must have been either ground-state NO^{2+}

TABLE V. Values of kinetic energy release T for $NO^{2+} \rightarrow N^+ + O^+$.

Observed process	Time window	T(eV)	A.E.(eV)	Exptl. method	References
$NO^{2+} \rightarrow O^+(+N^+)$, unimolec.	~2–4 μs	6.1		Metastables	Present work
$NO^{2+} \xrightarrow{He} O^+(+N^+)$	0–2 μs after collision	6.1 8.1		Collision	Present work
$NO^{2+} \xrightarrow{He} N^+(+O^+)$	0–2 μs after collision	6.2 8.2	Lower Higher	Collision	Present work
$NO^{2+} \rightarrow O^+(+N^+)$	~2–4 μs	6.15		Metastables	8
$NO^{2+} \rightarrow N^+ + O^+$	~0–3 μs	~8.5	40.3	Coincidence	13

ions, or excited states stable with respect to both radiative decay and internal conversion processes. The lack of agreement between the double-charge-transfer[25] and kinetic-energy-loss[37] measurements must be at least partly due to the fact that the latter[37] detect only nondissociative transitions. It was noted in the original work[37] that the kinetic-energy-loss data are in better agreement with the theoretical potential curves of Hurley[27] than with more recent[38] *a priori* calculations on doublet states of NO^{2+}. The latter employed methods analogous to those discussed above[28,33] for N_2^{2+} and for O_2^{2+}, and were shown[38] to account well for the double-charge-transfer results.[25]

The information summarized in Table V describes energy differences between dissociating levels and dissociation limits. The delayed predissociation with $T = 6.1$ eV (Table V) is consistent with tunneling predissociation of either the $X\,^2\Sigma^+$ state or $A\,^2\Pi$ state given by Hurley,[27] if only the energy requirement is considered. (If the more recent *a priori* calculations are considered, only the $X\,^2\Sigma^+$ state is appropriate.) However, the critical regions near the potential maxima are not accessible by Franck–Condon transitions from the ground state of NO. This Franck–Condon problem applies also to the collision-induced dissociation with $T = 8.1$ eV (Table V), which is reasonably consistent with $T = 7.4$ eV predicted for tunneling predissociation of the $B\,^2\Sigma^+$ state to $N^+(^2P) + O^+(^2D)$ on the basis of the potential curves due to Hurley.[27] According to the more recent *a priori* calculations,[38] the $B\,^2\Sigma^+$ state is repulsive in the Franck–Condon region, the appropriate intersection lying some 6.2 eV above the dissociation limits. This affords an alternative interpretation of the unimolecular spectrum in Fig. 8. This peak was extremely weak, and was observed only when every available experimental parameter, including pressure of NO in the ion source, was maximized. It is possible that this very weak unimolecular peak (Fig. 8) was in fact induced by collisions with the residual background pressure of NO in the first field-free region. If this interpretation is correct, the $B\,^2\Sigma^+$ state predicted more recently[38] can account for both the observed value of T and for the Franck–Condon requirements. Further, the repulsive $D\,^2\Pi$ state predicted by the same *a priori* calculations[38] affords the basis for a reasonable interpretation of the process (Table V) with $T = 8.1$ eV.

In summary, our understanding of the NO^{2+} ion leaves much to be desired. While the double-charge-transfer spectra,[25] appearance energy measurements[36] and kinetic energy release results (Table V) appear to be susceptible to a broad interpretation in terms of the available *a priori* calculations,[38] the kinetic-energy-loss experiments[37] and Auger spectra[18,20] present considerable problems of interpretation within the above picture. Neither of the available theoretical approaches[27,38] dealt with quartet states, and possibly some of the discrepancies could be explained on such a basis. However, it seems unlikely that the ground state of NO^{2+} could be a quartet state, so the observation in the Auger spectra[18,20] of a state of NO^{2+} at least 2 eV below the electron-impact onset is probably not thus explicable. Possibly this observation corresponds to the Auger analog of a "hot band", i.e., vibrational excitation of the intermediate K-hole ion, as suggested previously[5] for the case of CO.

CONCLUSIONS

The experimental results reported here provide new information on the species N_2^{2+}, O_2^{2+}, and NO^{2+}, which will have to be accounted for in any description of these di-cations. The energy resolution achieved in the present work ($\sim$0.1 eV) is not exceptional by present-day standards, but does appear to be superior to that obtained in any previous IKES study of these species. The present discussion of all experimental information on these species underlines the necessity for high-level *a priori* theoretical calculations of their electronic states. The work of Taylor[29] on N_2^{2+} provides an important start in this direction, and results of similar calculations on CH^{2+} and CO^{2+}, due to Wetmore, are presently being extended to include other diatomic di-cations. In view of the almost complete absence of optical spectroscopic information, this more indirect approach offers the only available means to an understanding of these species.

ACKNOWLEDGMENT

This work was supported financially by the Natural Sciences and Engineering Research Council of Canada.

[1] G. Herzberg, *Spectra of Diatomic Molecules*, 2nd. ed. (Van Nostrand, Princeton, 1950).
[2] K. P. Huber and G. Herzberg, *Spectroscopic Constants of Diatomic Molecules* (Van Nostrand, Princeton, 1979).
[3] J. M. Curtis and R. K. Boyd, J. Chem. Phys. **80**, 1150 (1984).
[4] R. W. Wetmore, R. J. Le Roy, and R. K. Boyd, Chem. Phys. (in press).
[5] R. W. Wetmore, R. J. Le Roy, and R. K. Boyd, J. Phys. Chem. (in press).
[6] R. G. Cooks, J. H. Beynon, R. M. Caprioli, and G. R. Lester, *Metastable Ions* (Elsevier, Amsterdam, 1973).
[7] M. Cobb, T. F. Moran, R. F. Borkman, and R. Childs, J. Chem. Phys. **72**, 4463 (1980).
[8] J. H. Beynon, R. M. Caprioli, and J. W. Richardson, J. Am. Chem. Soc. **93**, 1852 (1971).
[9] J. L. Franklin and M. A. Haney, in *Recent Developments in Mass Spectrometry*, edited by K. Ogata and T. Hayakawa (University of Tokyo, Tokyo, 1970), p. 909.
[10] W. Schultz, B. Meierjohann, W. Seibt, and H. Ewald, in *Recent Developments in Mass Spectrometry*, edited by K. Ogata and T. Kayakawa (University of Tokyo, Tokyo, 1970), p. 939.
[11] L. Deleanu and J. A. D. Stockdale, J. Chem. Phys. **63**, 3898 (1975).
[12] J. A. D. Stockdale, J. Chem. Phys. **66**, 1792 (1977).
[13] B. Brehm and G. de Frenes, Int. J. Mass Spectrom. Ion Phys. **26**, 251 (1978).
[14] A. K. Edwards and R. M. Wood, J. Chem. Phys. **76**, 2938 (1982).
[15] F. H. Dorman and J. D. Morrison, J. Chem. Phys. **39**, 1906 (1963).
[16] T. D. Mark, J. Chem. Phys. **63**, 3731 (1975).
[17] J. H. Agee, J. B. Wilcox, L. E. Abbey, and T. F. Moran, Chem. Phys. **61**, 171 (1981).
[18] K. Siegbahn, C. Nordling, G. Johansson, J. Hedman, P. F. Heden, K. Hamrin, U. Gelius, T. Bergmark, L. O. Werme, R. Manne, and Y. Barr, *ESCA Applied to Free Molecules* (North-Holland, Amsterdam, 1969).
[19] D. Stalherm, B. Cleff, H. Hillig, and W. Mehlorn, Z. Naturforsch. Teil A **24**, 1728 (1969).
[20] W. E. Moddeman, T. A. Carlson, M. O. Krause, and B. P. Pullen, J. Chem. Phys. **55**, 2317 (1971).
[21] P. K. Carroll, Can. J. Phys. **36**, 1585 (1958).
[22] P. K. Carroll and A. C. Hurley, J. Chem. Phys. **35**, 2247 (1961).
[23] L. de Reilhac and N. Damany, J. Phys. (Paris) Colloq. **32**, C4–32 (1971).
[24] L. de Reilhac and N. Damany, J. Quant. Spectrosc. Radiat. Transfer **18**, 121 (1977).
[25] J. Appell, J. Durup, F. C. Fehsenfeld, and P. Fournier, J. Phys. B **6**, 197 (1973).
[26] A. C. Hurley and V. W. Maslen, J. Chem. Phys. **34**, 1919 (1961).
[27] A. C. Hurley, J. Mol. Spectrom. **9**, 18 (1962).

[28]E. W. Thulstrup and A. Andersen, J. Phys. B **8**, 965 (1975).
[29]P. R. Taylor, Mol. Phys. **49**, 1297 (1983).
[30]J. Durup, in *Recent Developments in Mass Spectrometry*, edited by K. Ogata and T. Hayakawa (University of Tokyo, Tokyo, 1970), p. 921.
[31]H. Yamaoka, P. Dong, and J. Durup, J. Chem. Phys. **51**, 3465 (1969).
[32]N. R. Daly and R. E. Powell, Proc. Phys. Soc. **90**, 629 (1967).
[33]N. H. F. Beebe, E. W. Thulstrup, and A. Andersen, J. Chem. Phys. **64**, 2080 (1976).
[34]F. H. Dorman and J. D. Morrison, J. Chem. Phys. **35**, 575 (1961).
[35]A. S. Newton and A. F. Sciamanna, J. Chem. Phys. **50**, 4868 (1969).
[36]Y. B. Kim, K. Stephan, E. Mark, and T. D. Mark, J. Chem. Phys. **74**, 6771 (1981).
[37]A. O'Keefe, A. J. Illies, J. R. Gilbert, and M. T. Bowers, Chem. Phys. **82**, 471 (1983).
[38]P. W. Thulstrup, E. W. Thulstrup, A. Andersen, and Y. Ohrn, J. Chem. Phys. **60**, 3975 (1974).